

See discussions, stats, and author profiles for this publication at: <https://www.researchgate.net/publication/41806042>

On the Existence of Negative Excess Isotherms for Argon Adsorption on Graphite Surfaces and in Graphitic Pores under Supercritical Conditions at Pressures up to 10,000 atm

ARTICLE *in* LANGMUIR · MARCH 2010

Impact Factor: 4.46 · DOI: 10.1021/la903549f · Source: PubMed

CITATIONS

15

READS

13

4 AUTHORS, INCLUDING:



Duong Do

University of Queensland

493 PUBLICATIONS 9,817 CITATIONS

[SEE PROFILE](#)



Chunyan Fan

Curtin University

35 PUBLICATIONS 203 CITATIONS

[SEE PROFILE](#)



David Nicholson

University of Queensland

294 PUBLICATIONS 4,541 CITATIONS

[SEE PROFILE](#)

On the Existence of Negative Excess Isotherms for Argon Adsorption on Graphite Surfaces and in Graphitic Pores under Supercritical Conditions at Pressures up to 10,000 atm

D. D. Do,* H. D. Do, Chunyan Fan, and D. Nicholson

School of Chemical Engineering, University of Queensland, St. Lucia, Qld 4072, Australia

Received September 21, 2009. Revised Manuscript Received November 3, 2009

In this paper, we consider in detail the computer simulation of argon adsorption on a graphite surface and inside graphitic slit pores under supercritical conditions. Experimental results in the literature for graphitic adsorbents show that excess isotherms pass through a maximum and then become negative at high pressures (even for adsorption on open surfaces) when a helium void volume is used in the calculation of the excess amount. Here we show that, by using the appropriate accessible volume (which is smaller than the helium void volume), the excess isotherms still have a maximum but are always positive. The existence and the magnitude of this maximum is because the rate of change of the adsorbed density is equal to that of the bulk gas, which has a large change in bulk gas density for a small variation in pressure for temperatures not far above the critical point. However for temperatures far above T_c , this change in the bulk gas density is no longer significant and the maximum in the surface excess density becomes less pronounced and even disappears at high enough temperatures. The positivity of the adsorption excess persists for all pressures up to 10 000 atm for adsorption on surfaces and in slit pores of all sizes. For adsorption on a surface, the surface excess density eventually reaches a plateau at high pressures as expected, because the change in the adsorbed phase is comparable to that of the bulk gas. Positive excess lends support to our physical argument that the adsorbed phase is denser than the bulk gas, and this is logical as the forces exerted by the pore walls should aid to the compression of the adsorbed phase.

1. Introduction

The analysis of adsorption data involves various assumptions required in the calculation of the adsorption isotherm^{1,2} which we summarize below:

1. void volume is measured by the helium expansion method;
2. helium does not adsorb;
3. helium and adsorbate access the same set of pores;
4. and void volume does not change with loading and the adsorbent is inert

Many of these assumptions are not strictly correct, but for subcritical fluids they are unlikely to have any impact on the calculation as the adsorbed density is very much greater than the adsorptive density. However, for supercritical fluids or subcritical conditions close to the critical point, the adsorptive density may be significant compared to the adsorbate density and large errors can arise if care is not exercised in the calculation of adsorption isotherm. In recent years much effort has been spent on storage of high energy gases by adsorption technology. It is, therefore, important that we have the right tools to analyze adsorption problems in the most consistent and correct manner. This is the objective of the paper. Specifically, we consider adsorption of argon on a surface and in slit pores of different sizes to study the behavior of the excess isotherm and the local density distribution. But first let us briefly review what have been done in the literature.

Although adsorption of gases under subcritical conditions (usually at temperatures well below the critical point and above the triple point) has been well studied in the literature (see, for

example, refs 2 and 3), the study of supercritical adsorption is masked by the limitations of high pressure facilities and universal procedures to treat the data.^{4,5} The principal difficulties lie in the way we calculate the adsorption excess, or to be exact the way and the accuracy of determining the void volume in the adsorption cell. Why is the accuracy of the void volume so important? The answer is that because the density of the bulk gas phase is high it makes a greater contribution toward the total amount that is introduced into the adsorption cell.

Few experiments on supercritical adsorption have been carried out at extremely high pressures. Most studies are limited to about 20 MPa (200 atm or less) and only few experimental apparatus^{6,7} extend the range of pressures to as high as 650 MPa (6500 atm). It is unfortunate that early results were masked by the incorrect determination of void volume, resulting in very large negative excess.^{8,9} This was subsequently corrected with a better estimate of the void volume,¹⁰ which was obtained with helium expansion at very high temperatures to minimize any possibility of helium adsorption (which would overestimate the void volume). Gravimetric measurements of supercritical adsorption have been carried out with dedicated devices.^{11,12} These experiments and

*To whom correspondence should be addressed. E-mail: d.d.do@uq.edu.au. Fax: +61-7-3365-2789.

(1) Do, D. D. *Adsorption Analysis*; Imperial College Press: NJ, 1998.

(2) (a) Gregg, S. J.; Sing, K. S. W. *Adsorption, Surface Area and Porosity*; Academic Press: London, 1982. (b) Rouquerol, J.; Rouquerol, F.; Sing, K. *Adsorption in Porous Solids*; Academic Press: New York, 1999.

(3) Sircar, S. *Ind. Eng. Res.* **1999**, 38, 3670.

(4) Zhou, L. *Adsorption: Progress in Fundamental and Application Research*; World Scientific Press: NJ, 2007.

(5) (a) Salem, M.; Braeuer, P.; Szombathely, M.; Heuchel, M.; Harting, P.; Quitzsch, K.; Jaroniec, M. *Langmuir* **1998**, 14, 3376. (b) Myers, A. L.; Monson, P. A. *Langmuir* **2002**, 18, 10261.

(6) Vidal, D.; Malbrunot, P.; Guengant, L.; Vermesse, J.; Bose, T. K.; Chahine, R. *Rev. Sci. Instrum.* **1990**, 61, 1314.

(7) Malbrunot, P.; Vidal, D.; Vermesse, J. *Rev. Sci. Instrum.* **1993**, 64, 1984.

(8) Malbrunot, P.; Vidal, D.; Vermesse, J.; Chahine, R.; Bose, T. K. *Langmuir* **1992**, 8, 577.

(9) Vermesse, J.; Vidal, D.; Malbrunot, P. *Langmuir* **1996**, 12, 4190.

(10) Malbrunot, P.; Vidal, D.; Vermesse, J.; Chahine, R.; Bose, T. K. *Langmuir* **1997**, 13, 539.

(11) Herbst, A.; Germanus, J.; Harting, P. *J. Therm. Anal. Calorim.* **2000**, 62, 509.

(12) Dreisbach, F.; Losch, H.; Harting, P. *Adsorption* **2002**, 8, 95.

others have concentrated mostly on methane and hydrogen due to the importance of these gases as the high energy gases, which are vital for our civilization, although work has been done with other gases, such as noble gases, carbon dioxide, nitrogen, and higher hydrocarbons because of their interference with methane adsorption. A short survey of experimental work on supercritical adsorption was provided by Do and Do.¹³

Theoretical analysis of supercritical adsorption is done with classical methods as well as the modern tools of density functional theory (DFT), Monte Carlo (MC), and molecular dynamics simulations. These were developed to understand the various observations of what appear to be isotherms of excess adsorption, but which are in fact critically dependent on the estimation of the void volume. Let us proceed formally by listing below a number of “apparent” observations:

1. A maximum is observed in the plot of excess concentration versus either pressure or bulk gas density, usually occurring at pressures in the range of 1 to 10 MPa. This has been recognized for a very long time. Readers should refer to an excellent review of Menon.¹⁴ Others also observed this phenomenon.^{15–22}

2. The behavior of the excess concentration versus bulk gas density is linear in the pressure range beyond the pressure at which the maximum excess is observed.

3. When adsorption is very close to, but above, the critical point, the excess isotherm shows a very sharp spike at pressure close to the critical pressure, beyond which it decreases much more steeply than the rise of the spike. This is due to the sharp change in the bulk gas density for a very small variation in pressure close to the critical pressure. An example of this behavior is the adsorption of propane on graphitized carbon black²³ at $T = 97$ and 98°C (the critical temperature of propane is 96.8°C).

The classical tools of analysis of supercritical adsorption, for example equation of state or potential theory with quasi-vapor pressure concept, are not sufficient to shed any light on the mechanism of adsorption. This has prompted several studies with methods such as DFT and MC simulation. Monte Carlo simulation is the more powerful since it handles the statistical mechanics of adsorption and off-lattice particles accurately, whereas DFT entails approximations. Furthermore, molecules with shape are better handled with MC. We shall use this method here to shed more light on understanding supercritical adsorption; equally important is the choice of the accessible volume, which will be defined later and used to calculate the excess density.

2. Theory

Adsorption analysis of a volumetric experiment is carried out by introducing a known amount of gas, N , into the adsorption cell. The amount adsorbed is then taken as the difference between this amount and the amount that is left in the gas phase

$$N_{\text{ex}} = N - N_G \quad (1)$$

There is no problem in principle with the accurate measurement of amount N , introduced into the adsorption cell, but that

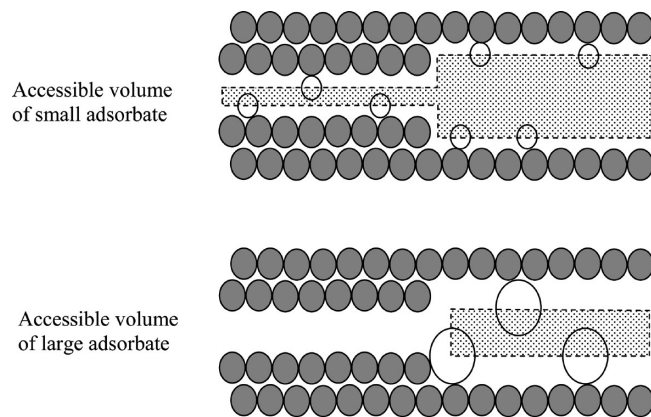


Figure 1. Accessible volumes probed by a small molecule and a large molecule.

cannot be said with the amount left in the gas phase, N_G . This is calculated as

$$N_G = V_G \rho_G \quad (2)$$

where ρ_G is the density in the gas phase at equilibrium, which can also be measured accurately. Thus, the principal issue in the calculation of the excess amount, N_{ex} , is the gas volume. To know this exactly, it is important that we define this volume in the most unambiguous manner. Although this is not so crucial for adsorption at subcritical temperatures well below the critical point, it can become very significant for supercritical adsorption and even for subcritical adsorption at temperatures close to the critical temperature.

Traditionally the void volume is measured by carrying out a helium expansion experiment, and the problems associated with this approach have been discussed regularly in the literature,^{2,3} and have been highlighted in the introduction. The most critical one is the overestimation of the actual volume occupied by the gas. Furthermore, different gases can occupy different spaces, and therefore it is important that one should determine the gas space that is occupied by the actual adsorptive. We refer to this as the accessible volume and stress that it is adsorbate dependent, since small adsorbates may probe some narrow pore spaces that large ones cannot and also because smaller adsorbates can access pore space closer to the wall than larger adsorbates. Our definition of an accessible volume, V_{acc} , as the volume in which a particle will have a nonpositive solid-fluid potential, and the corollary of this definition is that the boundary of the accessible volume is one that has zero solid-fluid potential energy.^{24,25} Figure 1 shows a schematic diagram of pores and the accessible volume probed by a small adsorbate molecule and a large adsorbate molecule. Here we show two representative pores, a small pore and a large pore. A small adsorbate can access both pores while the larger adsorbate only probes the larger pore (see the shaded region with a dashed line boundary). Furthermore, in the larger pore where both adsorbates have access the smaller one can approach closer to the surface atoms, resulting in a larger accessible volume for the small adsorbate in the larger pore. This illustrates our argument that the accessible volume can be adsorbate-dependent and is consistent with the well-known phenomenon of molecular sieving; some current theories in the literature take this into account (see for example ref 26). This simple example shows that the use of

(13) Do, D. D.; Do, H. D. *J. Chem. Phys.* **2005**, *123*, 084701.

(14) Menon, P. G. *Chem. Rev.* **1968**, *68*, 277.

(15) Ozawa, S.; Kusumi, S.; Ogino, Y. *J. Colloid Interface Sci.* **1976**, *56*, 83.

(16) Specovius, J.; Findenegg, G. H. *Bunsen-Ges Phys. Chem.* **1978**, *82*, 174.

(17) Suzuki, T.; Kobori, R.; Kaneko, K. *Carbon* **2000**, *38*, 630.

(18) Blumel, S.; Foster, F.; Findenegg, G. *J. Chem. Soc., Faraday Trans. II* **1982**, *78*, 1753.

(19) Findenegg, G.; Korner, B.; Fischer, J.; Bohn, M. *Ger. Chem. Eng.* **1983**, *6*, 80.

(20) Aranovich, G.; Donohue, M. J. *Colloid Interface Sci.* **1996**, *180*, 537.

(21) Zhou, L.; Zhou, Y. *Ind. Eng. Chem. Res.* **1996**, *35*, 4166.

(22) Murata, K.; Kaneko, K. *Chem. Phys. Lett.* **2000**, *321*, 342.

(23) Findenegg, G. H.; Loring, R. J. *J. Chem. Phys.* **1984**, *81*, 3270.

(24) Talu, O.; Myers, A. *AIChE J.* **2001**, *47*, 1160.

(25) Do, D. D.; Do, H. D. *J. Phys. Chem. B* **2006**, *110*, 17531.

(26) Nguyen, T. X.; Bhatia, S. K. *Langmuir* **2008**, *24*, 146.

helium volume for all gases is misleading and that it is not plausible that all gases can access the same space.

If the gas volume, V_G , in eq 2 is taken to be the one obtained from the helium expansion experiment, it is most likely that we will underestimate the excess amount because the helium-void volume often overestimates the space available to the actual adsorbate. If the helium-void volume is used to calculate the excess pore density, we have

$$\rho_{\text{ex}} = \frac{\langle N \rangle - V_{\text{He}} \rho_G}{V_{\text{He}}} \quad (3)$$

However, when we use the accessible volume as the basis for the calculation of the excess pore density we have

$$\rho_{\text{ex}} = \frac{\langle N \rangle - V_{\text{acc}} \rho_G}{V_{\text{acc}}} \quad (4)$$

The helium void volume overestimates the actual void volume because there will always be some helium adsorption which will be more significant in ultrafine pores. To avoid this problem, we replace the helium void volume in eq 3 by the absolute void volume, defined as the helium extrapolated to infinite temperature (a mathematical, not physical limit, as no material can exist at this temperature!). If the excess density based on the absolute void volume is negative, that based on helium void volume will be even more negative.²⁷

3. Results and Discussion

To exemplify some of the above issues we have carried out simulations of argon adsorption on a graphite surface and in graphitic slit pores at 298 K over a wide range of external pressures up to 10 000 atm. In these calculations, the graphite surface is represented by a standard one-dimensional 10-4-3 potential with no variation parallel to the surface. Slit pores of different size are used to study the effects of pore size on the behavior of the excess adsorbed phase. Slit pores are classified, depending on how many molecular layers can be packed within the pore. Pores having one layer are classified as ultrafine pores, and pores having more than three layers are called large pores while those in between these two categories are called intermediate pores. We begin by considering adsorption on an open surface.

3.1. Adsorption on a Graphite Surface. For adsorption on a surface, we carry out grand canonical Monte Carlo (GCMC) simulations for a very large slit pore such that the potential exerted by one wall does not overlap with that of the opposite wall, that is, adsorption on one wall is independent of that on the opposite wall. For the range of pressures studied in this paper under supercritical conditions, we find that a pore width of 20 times the collision diameter of argon (0.34 nm) is adequate, because up to 10,000 atm the adsorbate density only exceeds the gas phase density for about three molecular widths from the wall. Using one wall as a hard wall to simulate surface adsorption under supercritical conditions (a frequently used procedure) can lead to spurious results. This is not too important for adsorption at temperatures well below the critical point as the bulk gas density is very low, but for supercritical conditions the bulk gas density is very high and the density close to the hard wall differs from the gas phase density because the perfectly repulsive wall structures the adsorbate at the hard wall as seen in Figure 2. On the other hand, by using an appropriate large slit pore to simulate

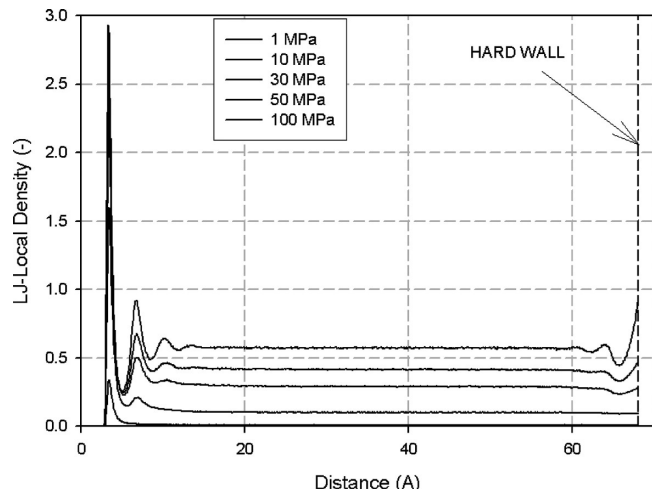


Figure 2. Local density versus distance for Ar adsorption at 298 K on a graphite surface with a hard wall at a distance of 68 Å from the graphite surface. The density increases with increasing pressure.

two independent surfaces, we observe the correct behavior as seen in the plot of the local density versus distance from one wall (Figure 3). The symmetry of the profile and the very large region of constant density in the center of the pore confirm that the two surfaces are independent with adsorbed phase near the walls and the bulk gas phase in the middle. The local density profiles next to one wall for this case of a very large slit pore match very well with those for the case where we use a hard wall at the top.

In dealing with adsorption on a surface, we cannot present the isotherm as an absolute isotherm because it depends very much on the box size. In the case of an extremely large box, the number of particles is very large and is mostly gas phase because of the high gas density under supercritical conditions. Therefore, it is appropriate that we consider the excess isotherm for surface adsorption and use the following definition for the surface excess density

$$\Gamma = \frac{\langle N \rangle - V_{\text{acc}} \rho_f}{2A} \quad (5)$$

where $\langle N \rangle$ is the GCMC ensemble average of the total number of particles in the simulation box, V_{acc} is the accessible volume, ρ_f is the bulk gas density, and A is the area of one wall.

Figure 4a shows the surface excess density of argon on a graphite surface at 298 K over the range of pressures up to 10 000 atm. From this figure and the plots of local density versus distance that we presented in Figure 3, a number of interesting observations can be made:

1. There is little detectable adsorption until the pressure reaches 10^5 Pa, much greater than under subcritical conditions. By comparison the surface excess density of argon adsorption at 87.3 K in Figure 4b, shows strong adsorption at 10 Pa.

2. The surface excess density has a maximum at a pressure which is greater than the critical pressure. This is because near this pressure the bulk fluid density exhibits a very large change for a very small variation in pressure.¹³ As temperature is increased further away from the critical point, the change in the gas density with a change in pressure is not as great as that when the temperature is in the neighborhood (but above) the critical point. In this case the maximum is less clear and eventually disappears as temperature is greater than 800 K (see Figure 4a).

3. The surface excess density decreases beyond the maximum point and finally decays to a positive plateau and finally increases further at very high pressures (see the inset of Figure 4a).

(27) Do, D. D.; Do, H. D. *J. Colloid Interface Sci.* **2007**, 316, 317.

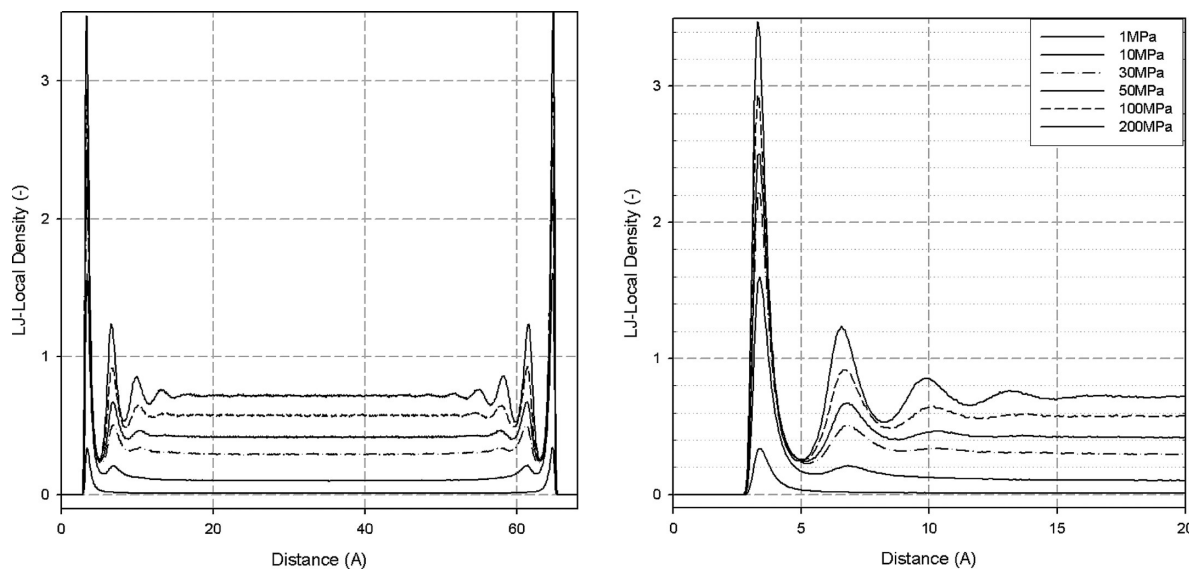


Figure 3. Plots of local density versus distance from one wall for the case of 68 Å slit pore at 298 K. The densities increase with increasing pressure.

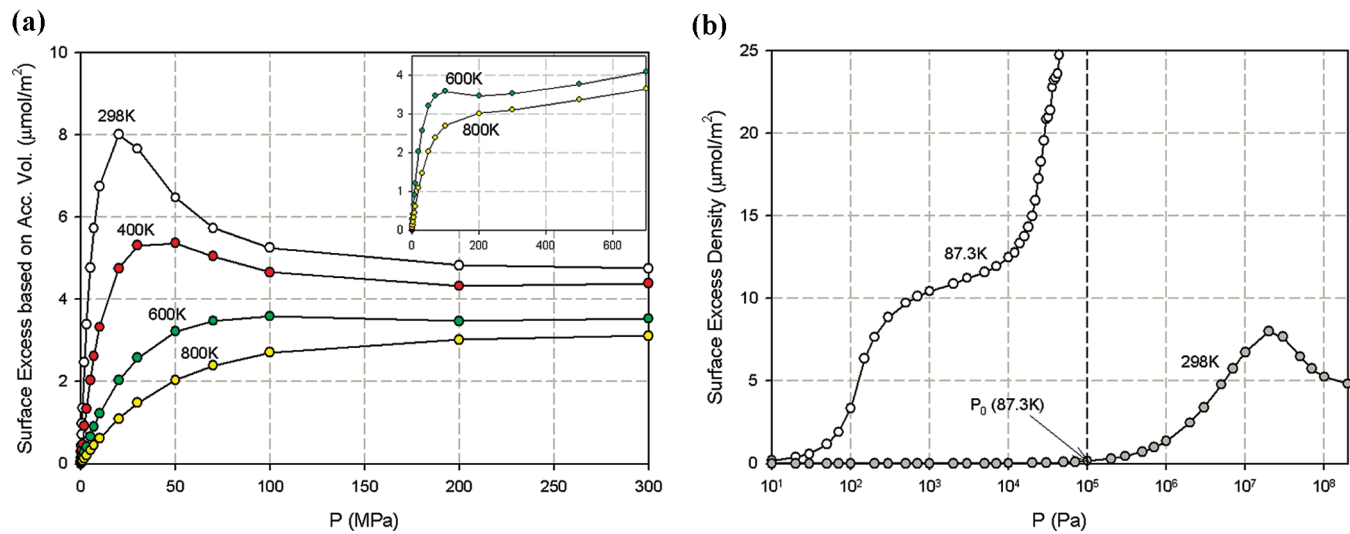


Figure 4. Surface excess isotherm of argon adsorption on a graphite surface at 298 K. (a) Linear scale; (b) semilog scale.

4. The plots of local density versus distance show a strong degree of delocalization due to the high thermal motion of particles compared to those for subcritical adsorption at 87.3 K (see Figure 5), where the distinct peaks result from strongly localized layer formation.

3.2. Ultrafine pores. *3.2.1. Slit Pore of 6.5 Å Width.* First we consider argon adsorption at 298 K in ultrafine graphitic pores. Here we take the 6.5 Å pore, which can only accommodate one layer under all conditions. The adsorption isotherm is shown in Figure 6.

We summarize a number of features of adsorption in this ultrafine pore.

1. The absolute isotherm increases monotonically with pressure and the rate of increase diminishes at very high pressure.

2. The excess isotherm (based on accessible volume) has a very shallow maximum, followed by a shallow minimum, and remains positive at all pressures. No clear maximum is observed for this ultra fine pore as shown in Figure 6b.

3. The bulk gas density is much lower than the absolute volumetric pore density (based on accessible volume).

4. Only a single molecular layer is possible (as seen in the local density plots versus distance from the pore wall in Figure 7b). The local density is completely confined to the region of non-positive solid-fluid potential energy (shown as dashed line in this figure).

5. The packing of molecules can be very efficient at very high pressure, as shown in Figure 7a. At low pressures less than 0.1 MPa (about 1 atm), the distribution of molecules is similar to that of a rarefied gas, but here they are confined in a two-dimensional space. As pressure is increased we see some degree of clustering, and finally at very high pressures we observe an approach to hexagonal packing, which is typical of adsorption under subcritical conditions. A comparison between the absolute adsorption isotherm at 87.3 K (subcritical conditions) and that at 298 K is shown in Figure 8. Apart from the early onset of adsorption at 87.3 K we see that the adsorbate density under supercritical conditions at very high pressures is actually greater than under subcritical conditions; that is the packing is facilitated by high external pressures. The greater mobility of argon particles at high temperatures makes the isotherm smoother than the 87.3 K

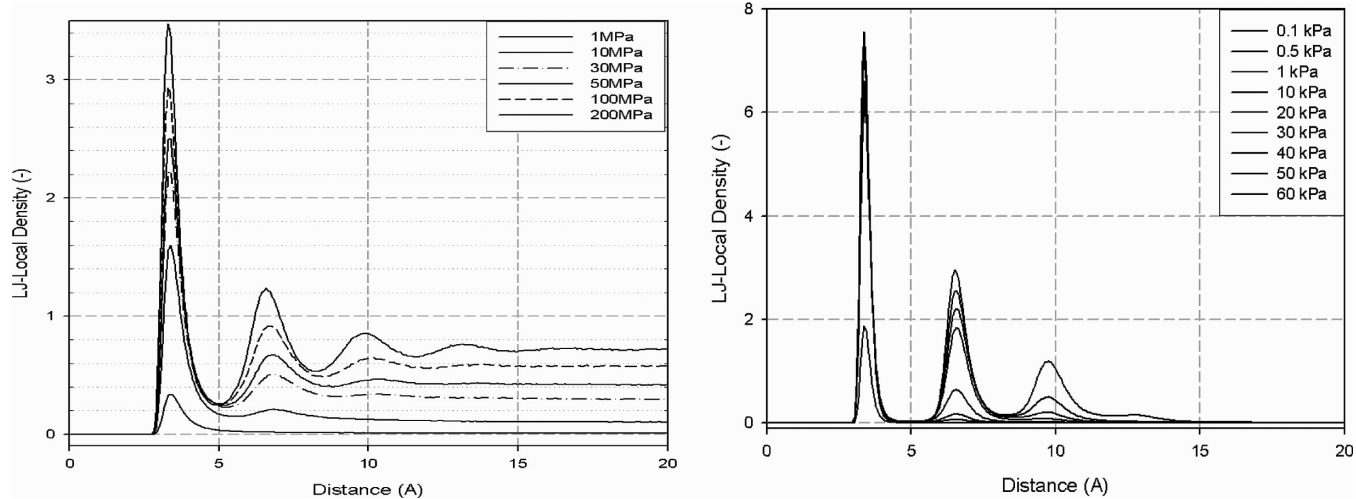


Figure 5. Local density versus distance from the surface for argon adsorption on graphite at 298 and 87.3 K. Densities increase with increasing pressure.

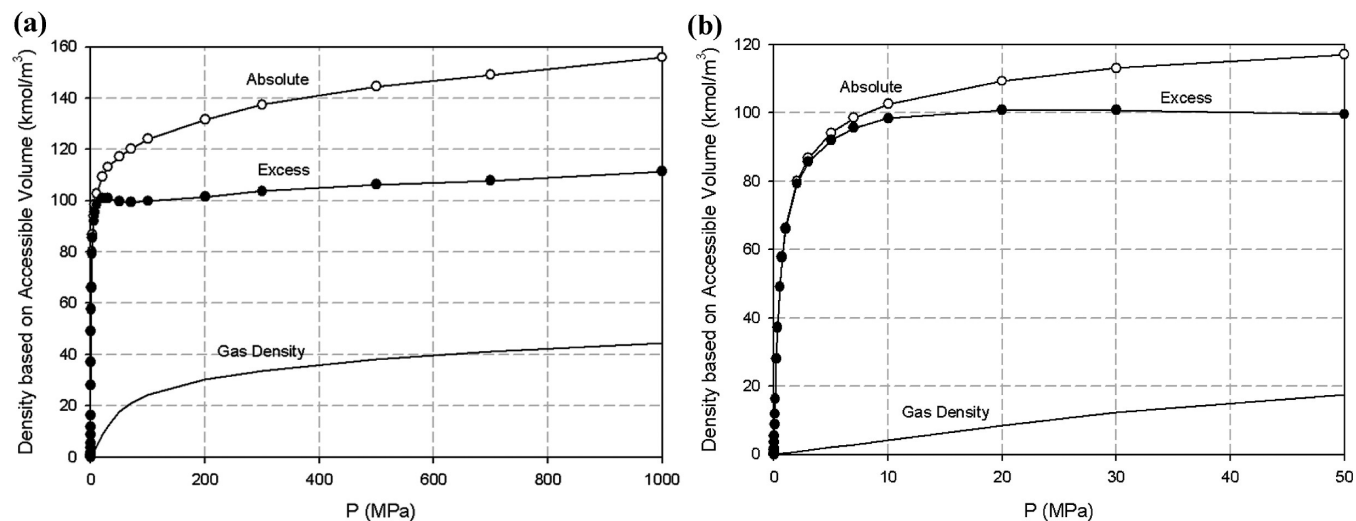


Figure 6. Isotherm of argon adsorption in 6.5 Å pore at 298 K. (a) Linear scale; (b) low pressure range in linear scale.

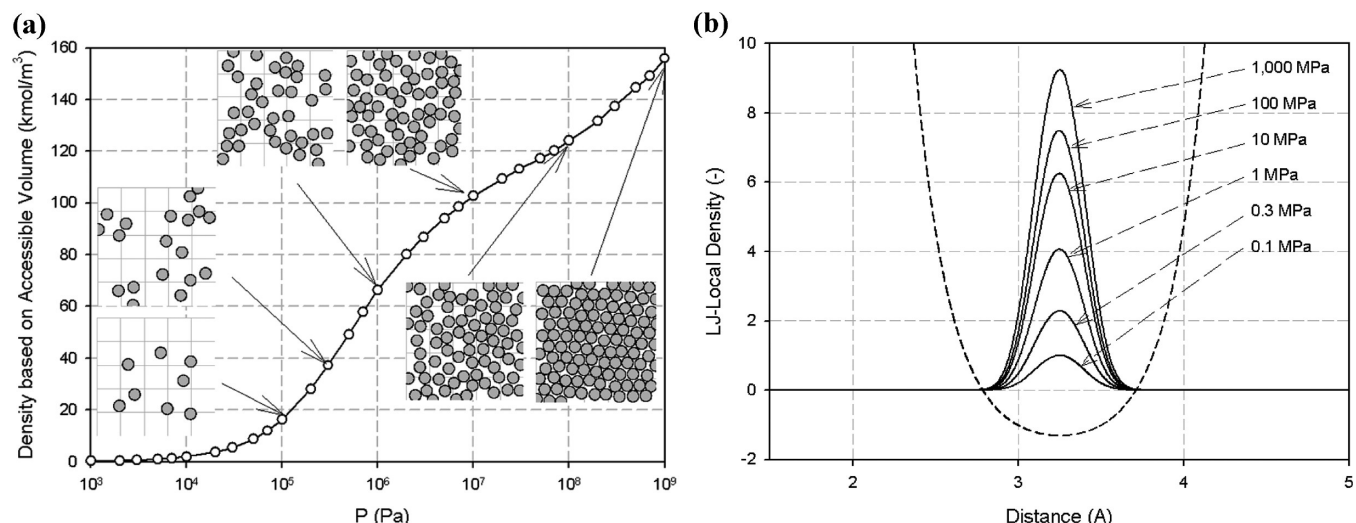


Figure 7. Adsorption isotherm of 6.5 Å pores. (a) Semilog scale; (b) local density plots versus distance from the wall.

isotherm. This is probably due to the existence of many similar local free energy minima.

One commonly assumed point about supercritical adsorption is that a plot of excess adsorption against the bulk gas density is linear.

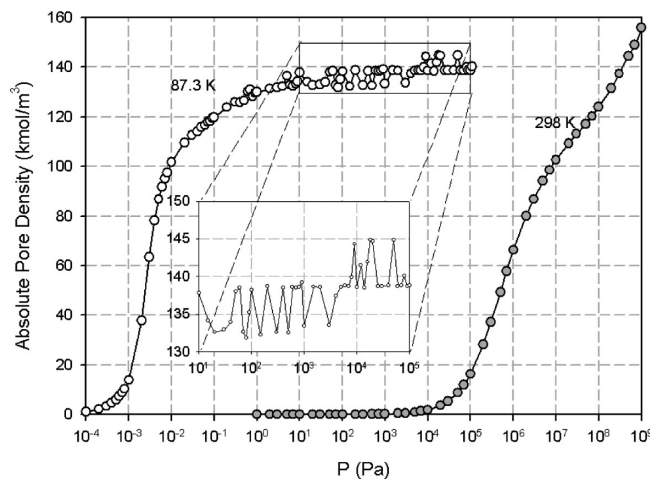


Figure 8. Comparison between the absolute adsorption isotherm of argon at 87.3 K and that at 298 K.

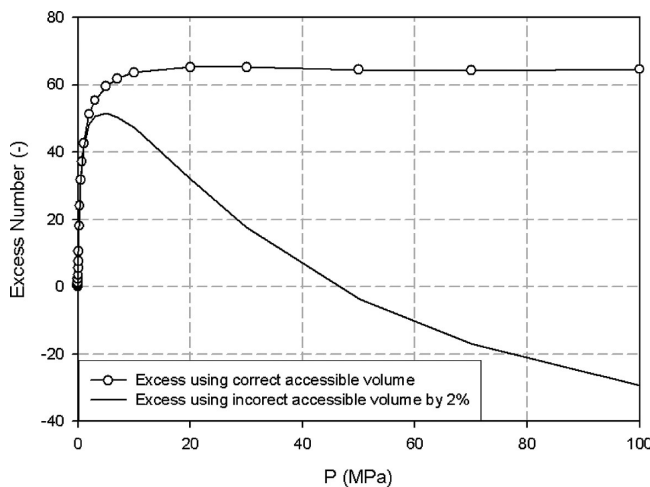


Figure 9. Plot of the excess isotherm versus pressure for argon at 298 K. The circle symbols are for the case when the correct accessible volume is used, and the solid line is for the case when the accessible volume is overestimated by 2%.

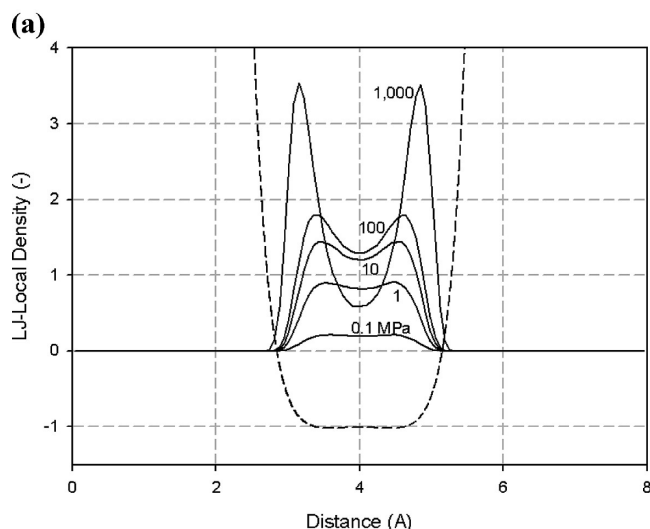


Figure 10. (a) Plots of local density versus distance for adsorption of argon in 8 Å graphitic slit pore at 298 K. (b) Adsorption isotherm of argon in 8 Å graphitic slit pore at 298 K.

This originates from the assumption that the amount in the pore has reached its saturation and any further increase in the bulk gas density would result in a linear decrease of the excess with a slope equal to the void volume (see eqs 1 and 2). We show in Figure 9 that when accessible volume is used, this is not the case. Experimentally we measure the number of moles in the adsorption cell and this quantity is the sum of the amount inside the pore and that outside the pore. To demonstrate this we have to obtain simulation data equivalent to experiment. We obtain this “simulated data” by assuring that the ratio of the pore volume to the adsorption cell volume is the same in both experiment and computer simulation. For a typical adsorption cell of 10 cm³ with 0.1 g of porous solid and a typical particle porosity of 0.33, the ratio of the pore volume to the adsorption cell volume is about 300. Thus given the computer data obtained from the GCMC simulation of argon adsorption in a single 6.5 Å pore, we can construct the number of particles in the adsorption cell (including those in the pores) as $N' = N + V_{cell}\rho_G$, where N is the number of particles in the single pore simulation.

For adsorption under supercritical conditions the amount contributed by the gas phase can be very significant. This means

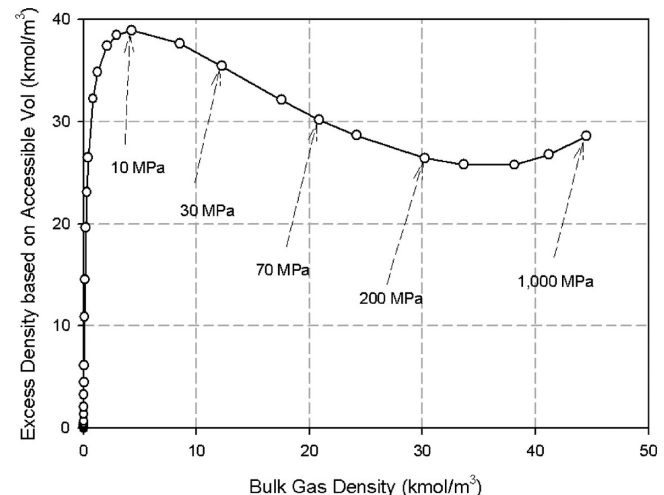
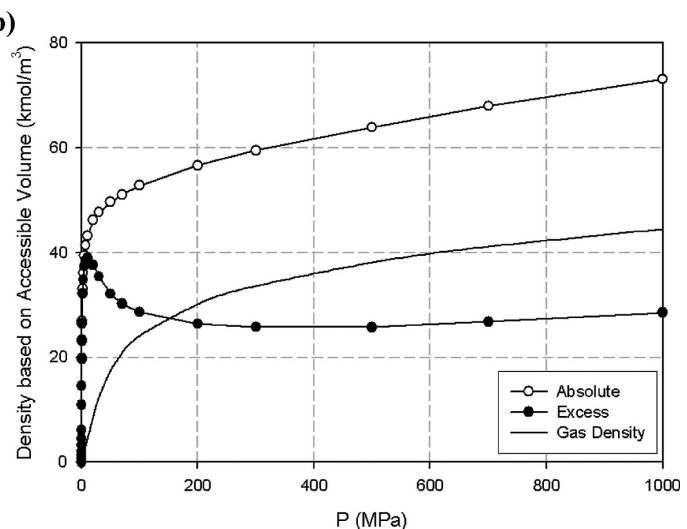


Figure 11. Plot of the excess density based on the accessible volume versus the bulk gas density for argon adsorption in 8 Å graphitic slit pore at 298 K.



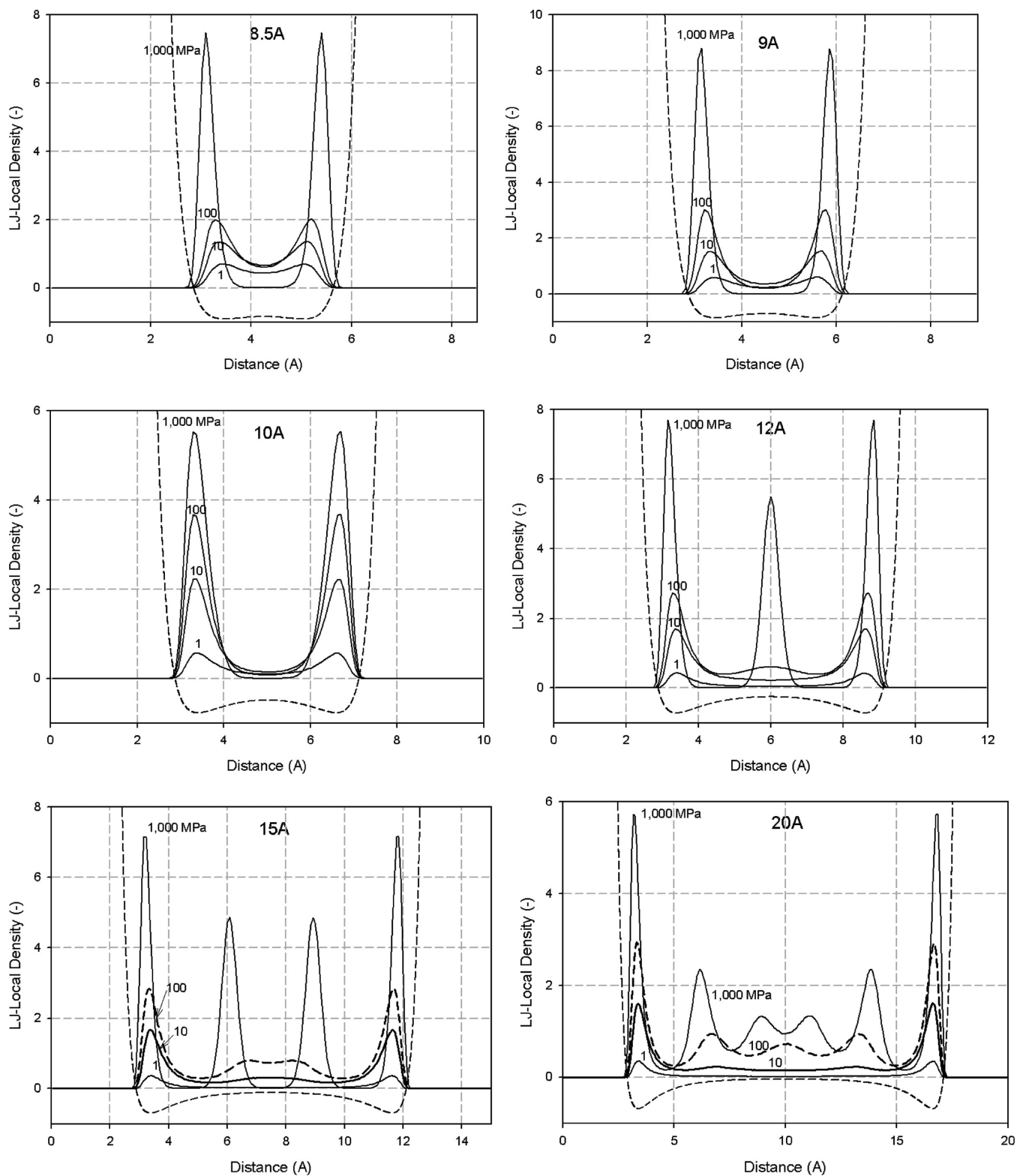


Figure 12. Local density plots versus distance for various graphitic slit pores, 8.5, 9, 10, 12, 15, and 20 Å.

that a small error made in the estimate of the void volume can make a very significant change in the calculation of the excess amount as we show in Figure 9, where the cell volume is of the order of 300 times greater than the accessible volume of the pore. Here we have plotted the excess amount as a function of pressure for the case where we use the correct accessible volume (unfilled circle symbols) and the case where the accessible volume is overestimated by a mere 2% (solid line). There is a significant

change in the way the excess amount behaves. This underlines the urgent need for techniques that determine the accessible volume as accurately as possible, or for a new way to present the adsorption isotherm of a supercritical fluid!

3.2.2. Slit Pore of 8 Å Width. As a second ultrapore we consider an 8 Å graphitic slit pore. Under moderate pressures and temperatures below the critical point this pore can accommodate one layer or two overlapping layers. For supercritical adsorption

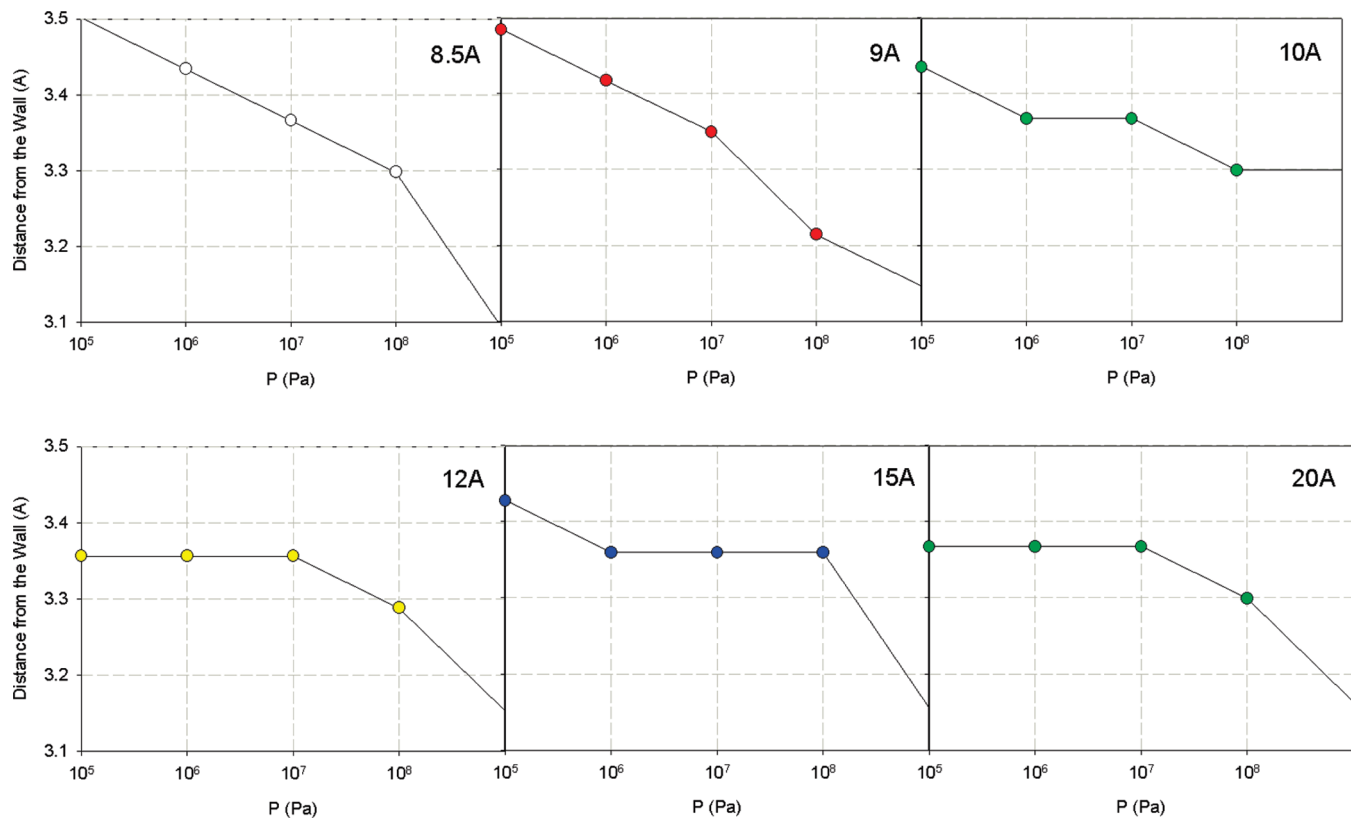


Figure 13. Shift in the first peak close to the surface as a function of pressure for 8.5, 9, 10, 12, 15 and 20 Å pores. Top three plots are for 8.5, 9, and 10 Å slit pores, while the bottom three are for 12, 15 and 20 Å pores.

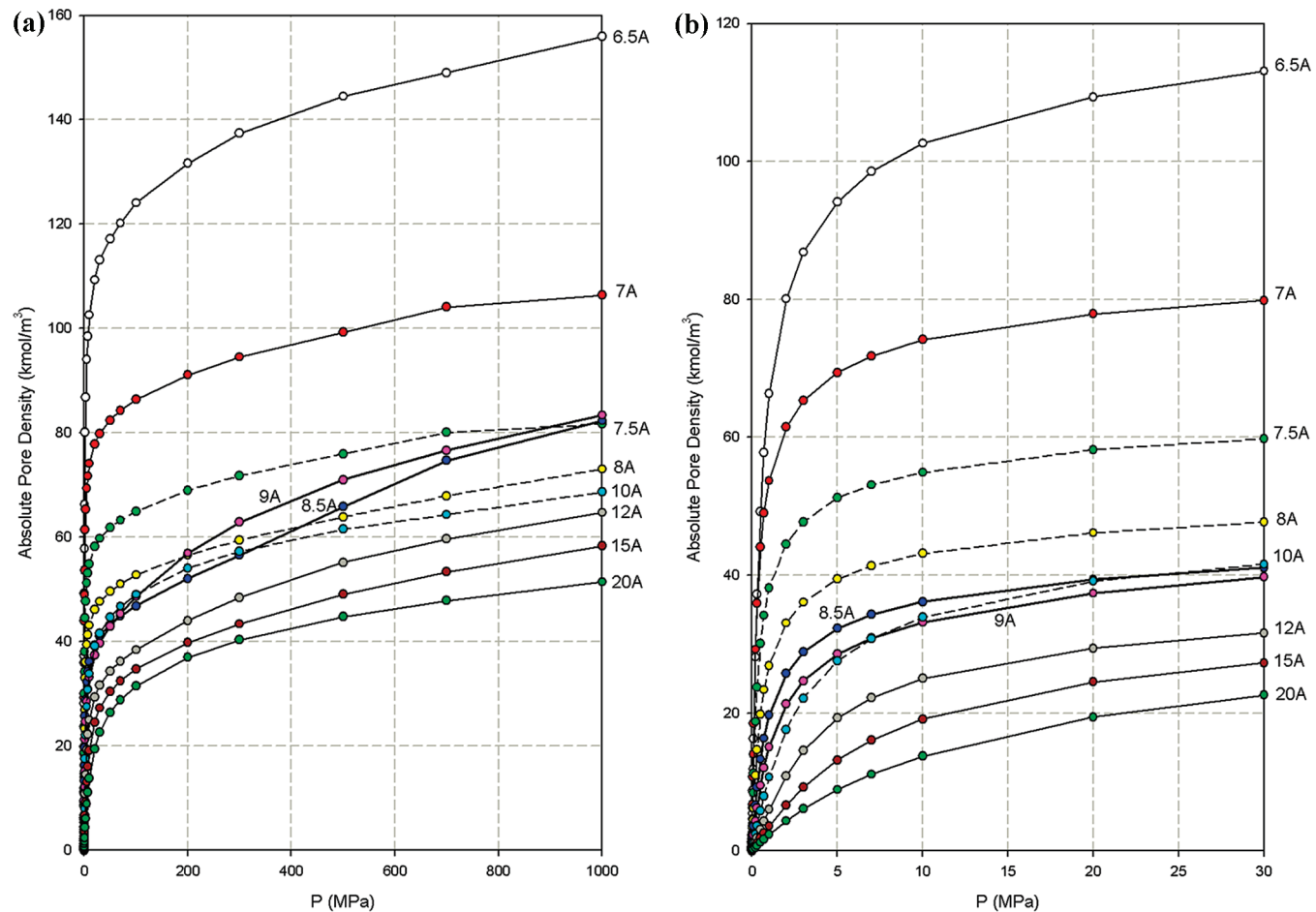


Figure 14. Plots of the absolute adsorption isotherms for all pores dealt with (a) wide range of pressure; (b) low range of pressure.

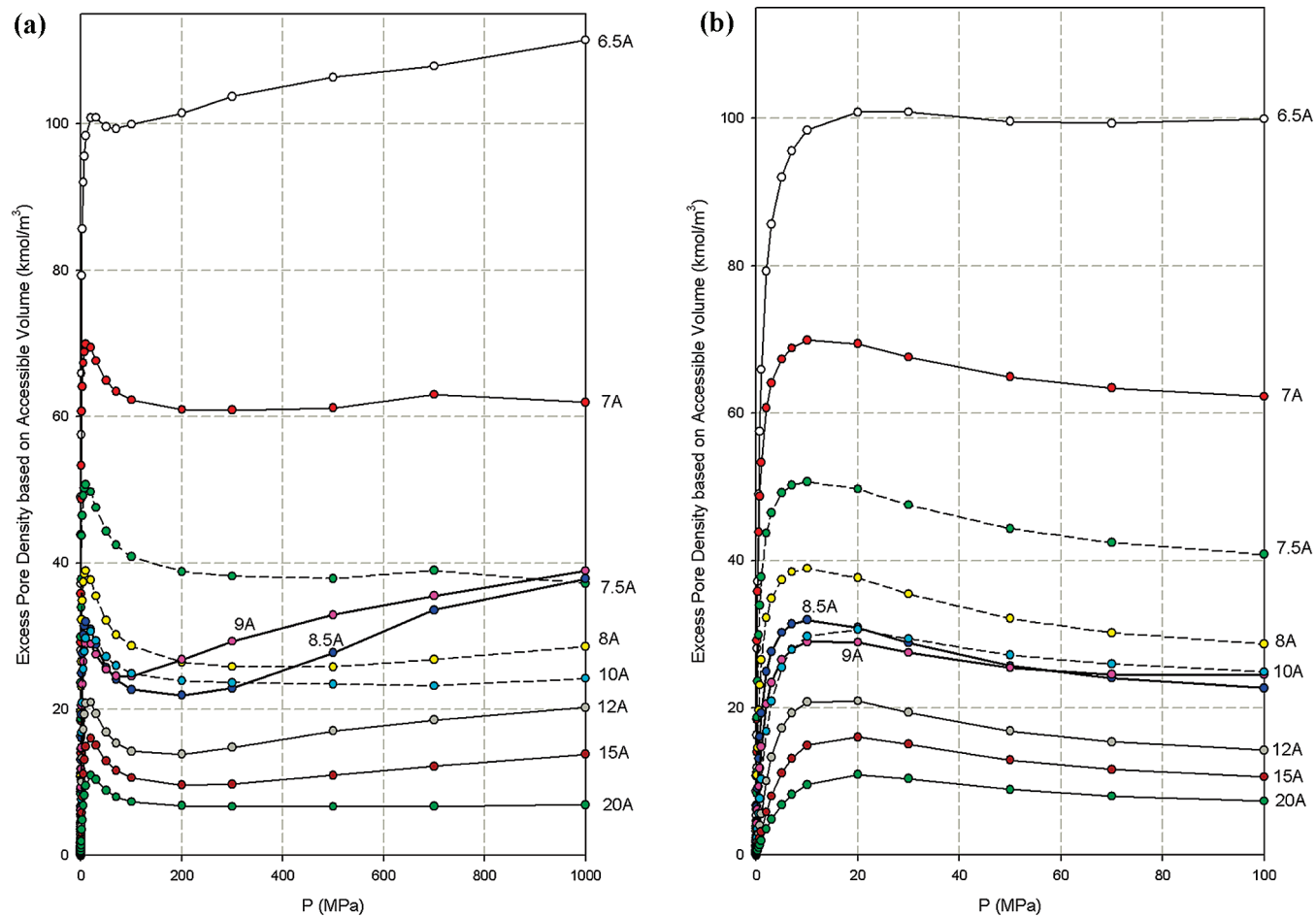


Figure 15. Plots of the excess adsorption isotherms for all pores dealt with (a) wide range of pressure; (b) low range of pressure.

where the pressure is very high, we observe the formation of two layers that extend into the repulsive region. This is seen in the plots of the local density against distance shown in Figure 10a, and we see the deconvolution of overlapping peaks at 1000 MPa into two distinct peaks that penetrate the repulsive region of the solid-fluid potential (shown as dashed line) when the repulsive force is balanced by the extremely high external pressure (1000 MPa). The adsorption isotherm for this pore is shown in Figure 10b. It is similar to that for the ultrafine 6.5 Å pore, except that in the 8 Å pore (and in larger pores) there is a clear maximum. Other features are similar to those observed in the 6.5 Å pore.

The plot of the excess density versus the bulk gas density is shown for this pore in Figure 11. Again we do not see linear behavior in the high pressure region, as often claimed in the literature. However, if we restrict the data to pressures less than 200 MPa (for example, due to the limitation of the experimental apparatus), we indeed observe linear behavior between 30 and 200 MPa. However, this is not due to saturation of the pore (see Figure 10b where we see the number of particles is steadily increasing), but rather to the fortuitous coincidence that the difference between the increase in the amount adsorbed and that of the bulk gas density results in linearity in this range of pressure.

3.3. Two and Higher Layers Pores. In studying of the two- and many-layer pores, we again arrive at the same conclusions as we did for ultrafine pores of 6.5 and 8 Å width. The major difference between all these pores lies in the behavior of the local density as a function of distance from a pore wall. As an illustration to this we show in Figure 12, the plots of local densities of 8.5, 9, 10, 12, 15, and 20 Å pores at 1, 10, 100, and 1000 MPa.

Pores are broadly classified as commensurate and incommensurate pores. The former term means that pores can pack an integral number of molecular layers at moderate pressures. Pores that are commensurate will show no or very little molecular penetration into the repulsive region of the solid-fluid potential, while incommensurate pores exhibit additional layers at very high pressures and penetration of particles into the repulsive part of the solid-fluid potential under extremely high external pressure.

A measure of the penetration can be seen in the shift of the layer adjacent to the pore walls. We take the 10 Å slit pore as an example. This is a commensurate pore as it can neatly pack two molecular layers at moderate pressures, and as pressure is increased we do not see any significant shift in the position of the peaks close to the pore walls. On the other hand, if we examine pores with widths, 8.5, 9, 12, 15, and 20 Å (all these are incommensurate) we see a shift of the peak closest to the pore wall as a consequence of the penetration into the repulsive region of the solid-fluid potential. The shift of the peak adjacent to the pore wall is plotted versus the pressure for the 10 Å pore and for these incommensurate pores in Figure 13. The 10 Å pore has the least shift and the 8.5 and 9 Å pores the largest, as the single particle density distribution evolves from one with overlapping peaks to one with two distinct peaks. This effect is also seen in the absolute adsorption isotherm, shown in Figure 14, where we see a sharp increase in the 8.5 and 9 Å isotherms when pressure is increased beyond 100 MPa, from where there is an evolution of two peaks (see Figure 12). This behavior is also seen with the plots of the excess pore density as a function of pressure for all pores, as shown in Figure 15.

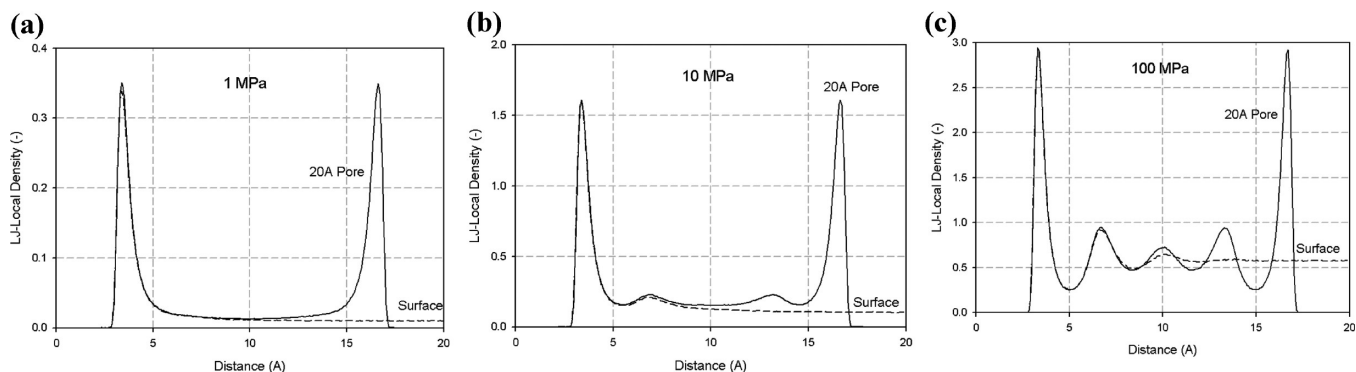


Figure 16. Local density plots in 20 Å graphitic slit pore and a graphite surface for argon adsorption at 298 K.

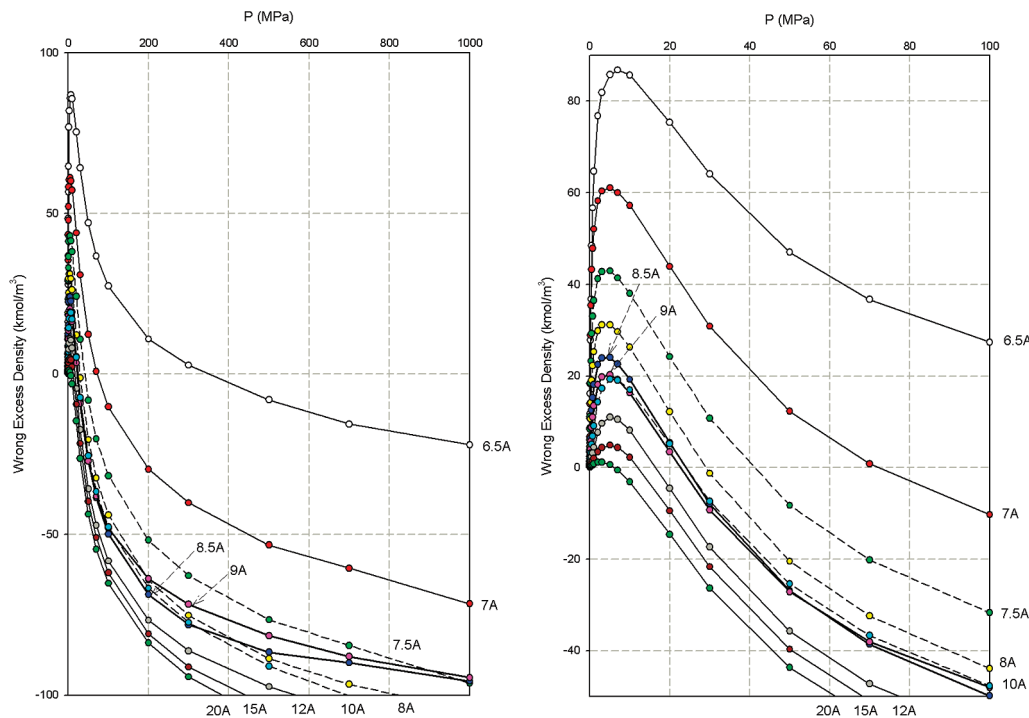


Figure 17. Plots of the incorrect excess density as a function of pressure for all pores dealt with in this paper.

3.3.1. How Large Is a 20 Å Pore from the Standpoint of Supercritical Adsorption. Let us now briefly study the local density plots for the 20 Å graphitic slit pore. This pore can pack about five molecular layers at high pressures, and as pressure is increased further we see six layers can be accommodated. At low pressures under which only one to two layers are formed on the surface of each pore wall, the adsorption in this 20 Å pore behaves very much like two independent surfaces. This is clearly seen in Figure 16 where we compare the local density plot for the 20 Å slit pore and for a graphite surface. At a pressure of 1 MPa when we have only one layer formed close to the surface, the behavior of the 20 Å slit pore is exactly the same as that of a surface (Figure 16a). When the pressure is increased to 10 MPa, we see the onset of the second layer the behavior of the two systems remains almost the same. Finally when we increase the pressure to 100 MPa, we see the formation of the fifth layer in the middle of the slit pore and only then does the adsorption in the 20 Å pore start to deviate from that of a graphite surface. Thus it can be concluded that a 20 Å pore can behave like two independent surfaces for pressures up to 10 MPa at this temperature. The practical implication is that if the experimental data for argon are available only up to 10 MPa (about 100 atm) the determination of

pore volume using supercritical fluids can only be reliable for pores having widths smaller than 20 Å.

3.4. Wrong Estimate of Void Volume in a Volumetric Adsorption Cell. Up to now our analysis has been carried out for simulation data in single pores. We now investigate the consequences of wrongly estimating the void volume in a typical adsorption cell described in Section 3.2.1. Again using a 1%-overestimated void volume in the calculation of the excess, we have

$$N_{\text{ex}}^{\text{Wrong}} = N' - (V_{\text{acc}}\rho_G + 303V_{\text{acc}}\rho_G) \quad (6)$$

Hence we derive the incorrect excess density as

$$\rho_{\text{ex}}^{\text{Wrong}} = \frac{N}{V_{\text{acc}}} - 4\rho_G \quad (7)$$

in which we have used $N' = N + V_{\text{cell}}\rho_G$ in eq 6. The first term on the RHS of the above equation is the absolute density. In Figure 17, we plot the wrong excess density for all pores that we have deal with so far, and we observe a complete change in the appearance of the excess isotherm, changing from a positive excess to a

negative excess when pressure is only very moderate. All pores show negative excess at high pressures, including the ultrafine pore of 6.5 Å width. The greater the pore width the sooner the excess isotherm becomes negative. Once more we stress that this calls for an urgent need for a new methodology to represent adsorption isotherms under supercritical conditions since a 1% experimental error in the estimation of the void volume is more likely than not.

4. Conclusions

In this paper, we have presented a detailed simulation study of adsorption of argon on a graphite surface and in graphitic slit pores under supercritical conditions and proposed that the accessible volume should be used in place of the helium void volume to calculate the excess amount adsorbed. With this choice, we have found that the excess isotherms have a maximum at a

pressure which is close to the critical pressure (P_c) for adsorption on a surface and is lower than P_c for pores of smaller width. The important point derived from this work is that using accessible volume, the excess isotherm remains positive for either surface adsorption or adsorption in pores of any size. Although this conclusion is true for argon adsorption in ideal systems, like flat graphite surfaces and graphitic slit pores, extrapolation of this to more complex systems must be treated with caution because, where the molecular packing might be very unfavorable, the adsorbed density could be less than the bulk fluid density. Additionally we have demonstrated that very small uncertainties in experimental data may lead to significantly erroneous interpretations of supercritical adsorption.

Acknowledgment. This work is supported by the Australian Research Council